

Increase in Contact Strength of Heavy-Loaded Rolling Bearings for Gear Drives and Transmissions

E. Tesker

Abstract Special rolling bearings are applied in layouts of various types of machine. The serviceability of these bearings greatly affects the main performance characteristics of power gears and gear drives. A special class of gear contains parts which are subjected to different advanced hardening treatment. The reason for the failure for such bearings is progressive contact fractures. Trouble spots for these fractures originate in sub-surface layers of the structurally non-homogeneous material obtained as a result of hardening treatment. In this relation, the study of kinetics and ways of generation of sub-surface (depth) contact failures is vital for the purpose of developing a method for analysis and an increase in the load-carrying capacity of the part under cyclic and dynamic loads. Trends of surface layer generation for heavy-loaded bearing parts of planetary turnover mechanisms (PTM) for mobile machines have been studied. The features of contact loading are revealed for parts of power gears with a surface hardened layer obtained through the use of various hardening treatments. Methods for depth contact stress analysis are proposed, design relations are obtained which allow for determining, in each specific case, the position of a risky zone where the trouble spots of fatigue depth fractures can appear. A method for analysis is proposed which permits determining the values of the hardened layer parameters necessary to provide high resistibility to contact fractures. Examples of the analysis of depth contact strength are given for the bearing parts of PTM for the mobile machine.

Keywords Rolling bearings • Hardened surface layers • Loading • Load-carrying capacity • Depth contact fracture • Way of fracture • Cyclic and dynamic loads • Contact fractures

E. Tesker (✉)
Volgograd State Technical University, Volgograd, Russia
e-mail: agromash-vlg@rambler.ru

1 Introduction

One of the key problems of advanced mechanical engineering is the increase in reliability and technical level of heavy-loaded gears and transmissions in which the shaft supports are the rolling bearings.

The practice of operation shows that the main reason for the insufficient serviceability of gears is the progressive contact fracture of operating surfaces.

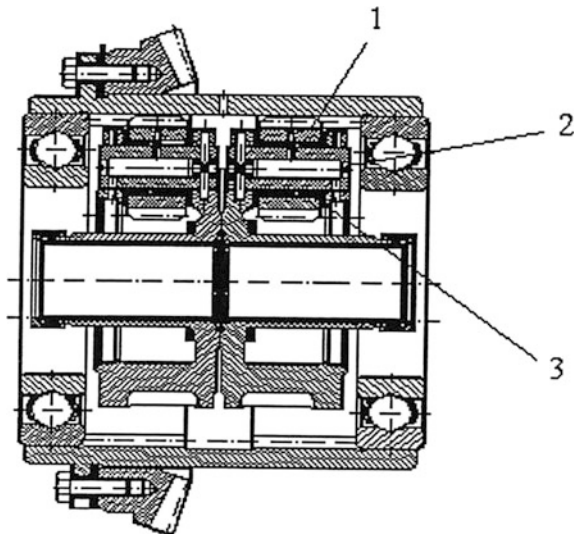
A special class comprises single-purpose bearings for gearboxes with parts that have been subjected to advanced hardening treatment. The reason for the failure of such bearings is progressive contact fractures. Trouble spots for these fractures originate in the very hardened layer or in the material core.

Analysis of conditions for generation of depth fractures and the development of methods for analysis of surface hardened parts are the vital problem, since the existing methods for design and analysis of the load-carrying capacity of surface hardened bearings do not fully consider the features of contact loading for parts with a structurally non-homogeneous surface hardened layers and kinetics and reasons for the generation of fatigue fractures.

2 Stressed State of Surface-Hardened Parts Under Contact Loads

The layout of the planetary turnover mechanisms (PTM) for the mobile machine has been chosen as the object of study (Fig. 1).

Fig. 1 Typical layout of PTM. 1 satellite, 2 satellite axis, 3 needle of the bearing

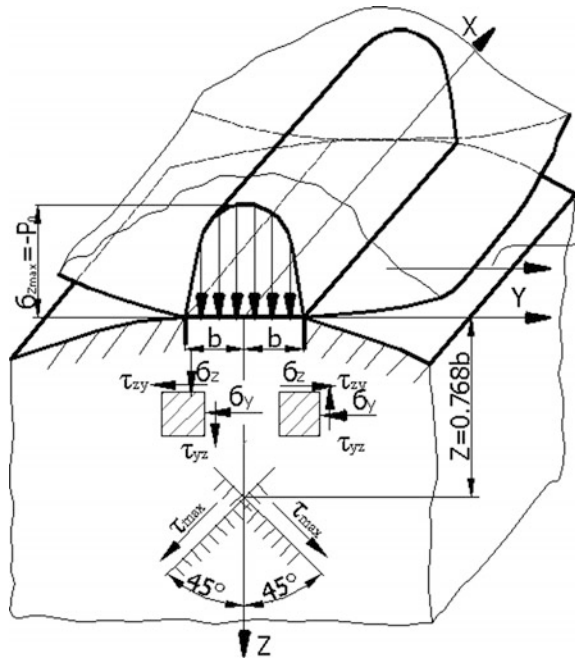


Analysis of the loaded state for parts of the bearing with cylindrical surfaces shows that, similar to the contact of two cylinders, the most loaded zone is not only the zone of the layer surface ($\sigma_z \text{ max} = p_0$), but also the deeper layers of the material located at a depth of $z = 0.786b$ from the surface of contact (Fig. 2).

Expressions for components of stresses $\sigma_x, \sigma_y, \sigma_z, \tau_{zy}, \tau_{zx}, \tau_{yx}$ at the boundaries of the contact area ($y \approx 0.8b$) are determined in accordance with formulas of the elasticity theory [1, 2]:

$$\begin{aligned}
 \sigma_x &= -p_0 2\mu \frac{z}{b} \left(\sqrt{\frac{b^2 + u}{u}} - 1 \right); \\
 \sigma_y &= -p_0 \frac{z}{b} \left(\sqrt{\frac{b^2 + u}{u}} \left(2 - \frac{b^2 z^2}{u^2 b^2 z^2} \right) - 2 \right); \\
 \sigma_z &= -p_0 \frac{bz^3}{u + b^2 z^2} \sqrt{\frac{b^2 + u}{u}}; \\
 \tau_{yz} &= -p_0 \frac{byz^2}{u^2 + b^2 z^2} \sqrt{\frac{u}{b^2 + u}}; \\
 \tau_{zx} &= \tau_{xz} = 0; \tau_{xy} = \tau_{yx} = 0,
 \end{aligned}
 \tag{1}$$

Fig. 2 Scheme of stresses at the contact of two cylinders



where b is the half width of the contact band; y is the coordinate of the point along the width of the contact area; z is the coordinate of the point along the depth; μ is the Poisson factor; and u is the maximum root of the equation

$$\frac{y^2}{b^2 + u} + \frac{z^2}{u} = 1. \tag{2}$$

In order to study the conditions for the contact interaction of heavy-loaded rolling supports of a PTM, and to create methods for analysis of the depth contact strength on its basis, a generalized mathematical model has been developed. This model is based on the fact that the load-carrying capacity of parts with a surface hardened layer is determined not only by distribution of equivalent tangential stresses with the distance from the surface to the considered point with the coordinate $z = z_i$, but also by the laws of variation of the contact endurance limits with regards to the thickness of the structurally non-homogeneous layer.

On this premise, one can state that the depth contact fractures will first appear at a certain distance from the contact surface $z_i = z_{min}$, in such zones where the value of the function of the safety factor $h(z)$ is a minimum, that is,

$$h(z) = \tau_k(z_{min}) / \tau_{eq}(z_{min}) \leq n_{min}. \tag{3}$$

Here, τ_k is the contact endurance limit for the hardened layer, and τ_{eq} are the equivalent tangential stresses determined in accordance with formulas of the elasticity theory.

The condition (3) is represented as a diagram demonstrating the law of variation of stresses and properties of the material along the depth of the surface layer of contacting parts (Fig. 3).

In order to obtain the relations $\tau_k(z)$, the laws of variation of micro-hardness along the thickness of the surface layer material have been studied. These surface layers have been obtained through the use of various surface hardening treatments

Fig. 3 Laws of variation of stresses and properties of the material along the length of the surface layer. 1 Distribution of contact endurance limits along the thickness of the layer (τ_k); 2 diagrams of equivalent stresses τ_{eq} ; $z = z_i$ —current coordinate and its corresponding values of equivalent stresses $\tau_{eq i}$

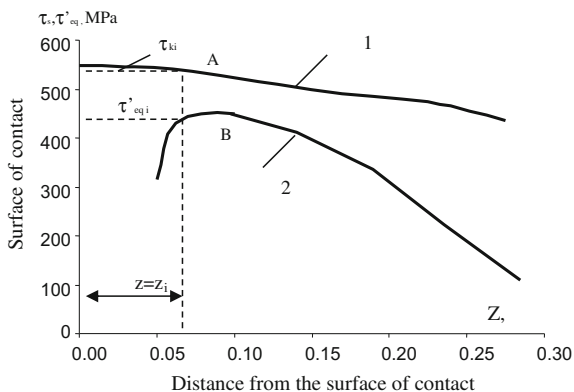
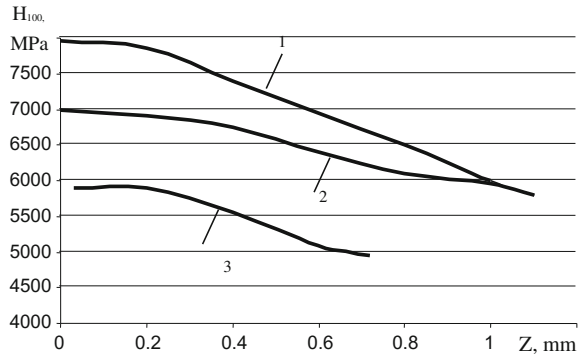


Fig. 4 Variation of micro-hardness along the thickness of case-hardened layers with different versions of hardening treatment. 1–3 Curved lines obtained through the formula (4). Points correspond to experimental values of the micro-hardness for local volumes



(case-hardening, nitro-carburizing, laser hardening, nitriding). The obtained curved lines of hardness distribution are shown in Fig. 4.

Relations (4–5), which were obtained after the processing of experimental data, describe the laws of hardness variation depending on the layer of thickness δ , and the hardness on the surface H_s and in the core H_c of the material of the bearing parts.

For case-hardened parts of bearings,

$$H = \frac{H_n}{\left(\frac{H_n}{H_c} - 1\right) \left(\frac{z}{\delta_c}\right)^2 + 1} \tag{4}$$

For parts of bearings treated by laser,

$$H = \frac{H_n}{\left(\frac{H_n}{H_c} - 1\right) \left(\frac{z}{\delta_c}\right)^4 + 1} \tag{5}$$

The root-mean-square relative error of design and experimental values does not exceed 6%; and the maximum deviations of the measured values from those of the design are within the ranges of $\pm|\delta|$.

When applying the developed model of the contact interaction of the surface-hardened parts of bearings, methods have been developed for analysis of the depth contact strength of bearings for transmissions under static and cyclic contact loads. In each specific case, the model and design relations allow for determining, through calculations, the coordinate $z = z_{\min}$, that is, the location of this risky zone where plastic deformations (under overloads) or trouble shots of fatigue cracks can appear.

3 Methodology for Analysis of the Depth Contact Strength of Surface Hardened Parts

The design model of the depth contact strength under cyclic loads is based on relations which characterize the variation of properties of the bearing material with the distance from the surface towards the material core, and also on equations determining the cyclic contact stresses which cause fatigue fractures in the surface layer.

At the interaction of two cylinders with parallel axes (Fig. 2), the tangential stresses $\tau_{zy}(\tau_{yz})$ hold the highest risk with regard to the appearance of sub-surface fractures. It is evident that these stresses act on areas which are parallel and perpendicular to axes z and y and separated from the plane of symmetry by the distance $y = \pm 0.85b$ (here, b is the half-width of the contact area). The maximum span of stress $\tau_{zy}(\tau_{yz})$ variation is at the boundaries of the contact area ($y = \pm b$) at a depth of $0.5b$. At this depth, the tangential stresses are $\tau_{zy} = \pm 0.25p_0$; and, therefore, the amplitude of these stresses is $\tau_{zy} = 0.5 p_0$ (where p_0 is the maximum normal contact stress acting along the axis of symmetry of the contact band). Equivalent tangential stresses τ_{eq} , which are determined by the equation given immediately below, are taken to be the strength criterion under the action of cyclic contact loads:

$$\tau_{eq} = \tau_{zy} + k\sigma_y. \quad (6)$$

The chosen strength criterion almost completely corresponds to advanced representations of the terms for the appearance of fatigue fractures. The fatigue strength at any point of the area of the part making contact (located at a certain distance z from the contact surface) will be determined in accordance with the relation of diagrams of cyclic stresses τ_{eq} and the surface endurance limit to be defined by the formula (7) (Fig. 5).

$$\tau_k(z) = cH(z). \quad (7)$$

Therefore, in accordance with the proposed model, for the case of cyclic contact loading of rolling bearings for transmissions and drives, the fatigue fractures first appear in the zone $z = z_{\min}$ with the lowest safety factor of cyclic strength n_{\min} . The coordinate $z = z_{\min}$ that determines the position of this zone can be found by the equation

$$\frac{d}{dz}n(z) = \frac{d}{dz} \left(\frac{\tau_k(z)}{\tau'_e(z)} \right) = 0. \quad (8)$$

Then, we have equations that describe the terms of the contact strength of bearings under cyclic loads for case-hardened parts:

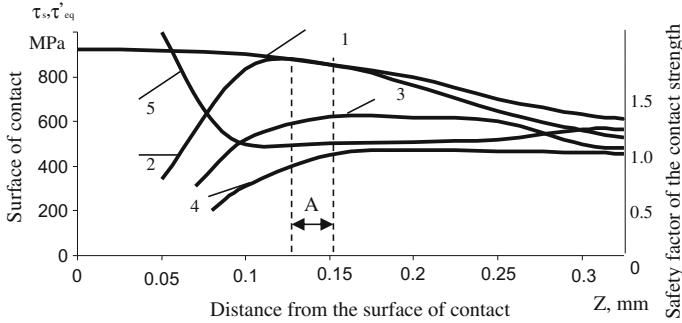


Fig. 5 Distribution of stresses under static loads and values of the safety factor of the contact strength n in different zones of the contacting surface: A the area ($n_{\min} \approx 1$) where contact fractures can appear at operation of bearings; 1 diagram of allowable stresses τ_s which are limited by the material yield point at different zones of the hardened layer; $2-4$ diagrams of equivalent stresses τ_{eq} for different diameters of rolling solids (needles) (4, 6, 16 mm, respectively); 5 diagram characterizing the laws of variation of the safety factor of the contact strength $n(z)$

$$\frac{d}{dz} \left(\frac{cH}{\left[\left(\frac{H_n}{H_c} - 1 \right) \left(\frac{z}{\delta_c} \right)^2 + 1 \right] (\tau_{xy} + k\sigma_y)} \right) = 0. \tag{9}$$

In the case of laser hardening,

$$\frac{d}{dz} \left(\frac{cH}{\left[\left(\frac{H_n}{H_c} - 1 \right) \left(\frac{z}{\delta_c} \right)^4 + 1 \right] (\tau_{zy} + k\sigma_y)} \right) = 0. \tag{10}$$

As an example, Fig. 6 shows the possible arrangement of curve lines $\tau_z(z)$ and $\tau_{eq}(z)$ calculated for the contact of real surfaces.

When analyzing the loading of the contact zone of bearing parts, it is necessary to consider cases of twist and mismatch that lead to a considerable increase in stresses determined by the elasticity theory (see Figs. 7, and 8).

At great values of angles of twist for rolling bodies and small values of convergence of contacting surfaces, the contact of parts takes place only at the portion of the contact line L (Fig. 8).

Figure 8 shows that even a small increase in the angle of twist leads to a considerable increase in loads on the bearing. That is why when determining the limiting allowable load acting on the bearing, the factor k_γ has been introduced. It accounts for the increase in contact pressure caused by the radial twist of rolling bodies. In order to determine the numerical values of this factor, the concept of the total factor of overload k_Σ has been introduced. It represents the product of factors

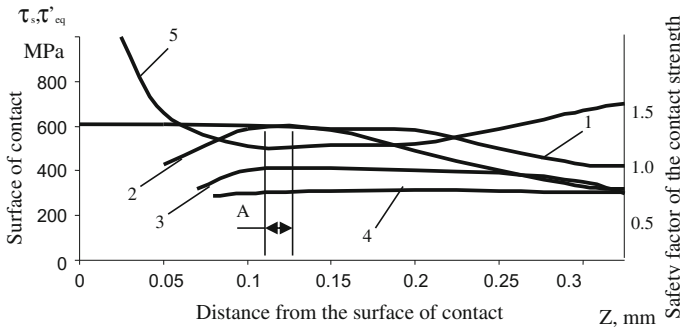
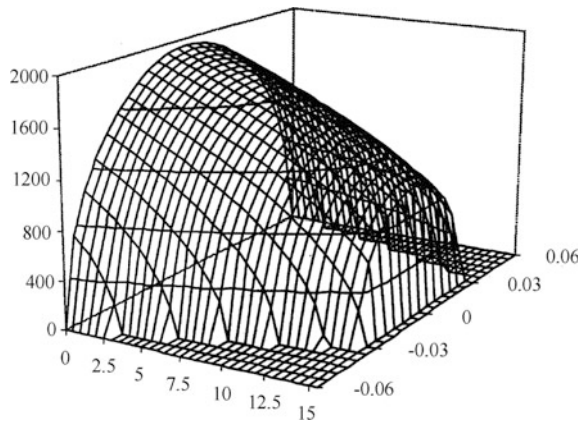


Fig. 6 Values of the safety factor of the contact strength (function $n(z)$) at different zones of the hardened surface layer (curve 5): A the area ($n_{\min} \leq 1$) where primary contact fractures can appear; 1 the diagram of allowable stresses $\tau_{k(z)}$; 2–4 diagrams of equivalent tangential stresses $\tau_{eq}(z)$ for different diameters of needles (4, 8, 16 mm, respectively)

Fig. 7 Distribution of normal contact stresses along the contact area for the angle of twist $\gamma = 0.00005$ rad



considering the dynamic loads in meshing of pinions for a PTM and the factors of non-uniform load distribution between satellites and non-uniform load distribution between rolling bodies in the bearing.

The influence of the angle of twist on the factor of overload is shown in Fig. 9.

An experimental study of the contact strength of bearing parts for a PTM of the mobile machine has been carried out during tests at the stand with the closed power circuit. In order to choose the testing modes, corresponding to real loading conditions, contact strength analysis of bearing parts for a PTM has been preliminarily performed by means of the methods developed for analysis of the depth contact strength. The values of parameters and factors involved in design formulas have been determined accounting for the features of design and operation of a PTM. The calculation results for specific conditions of contact loading are shown in Figs. 10 and 11.

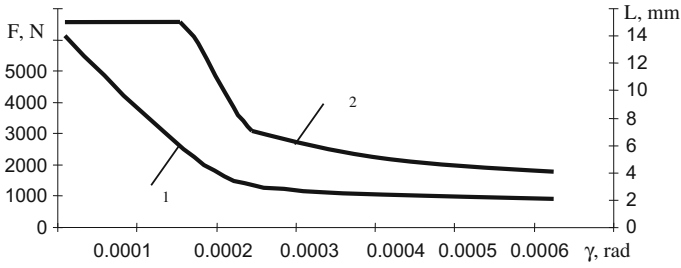


Fig. 8 Diagrams of variation for the ultimate force of the contact load (F) and the length of the contact line (L), depending on the angle of twist γ : 1 the ultimate force F ; 2 the length of the contact line L

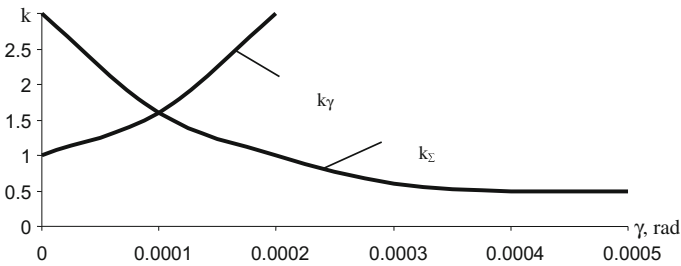


Fig. 9 Influence of the angle of mismatch γ on the value of the overload factor

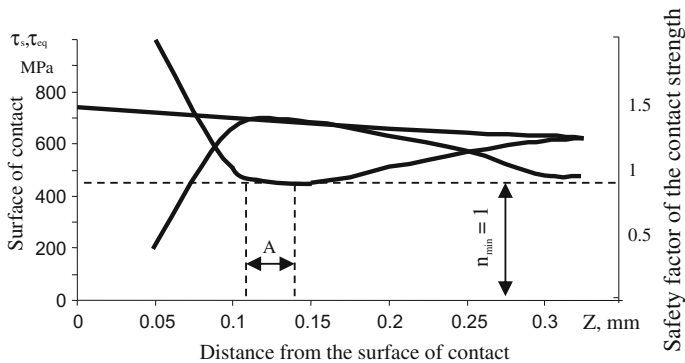


Fig. 10 Diagrams of stress distribution and properties of the material at the surface layer of bearing parts for a PTM under static loads (overloads) and the corresponding values of safety factors of the contact strength n in different zones of the contacting surface of case-hardened parts: 1 allowable stresses in accordance with the contact strength; 2 equivalent tangential stresses; 3 distribution of the safety factor of the contact strength along the thickness of the hardened layer

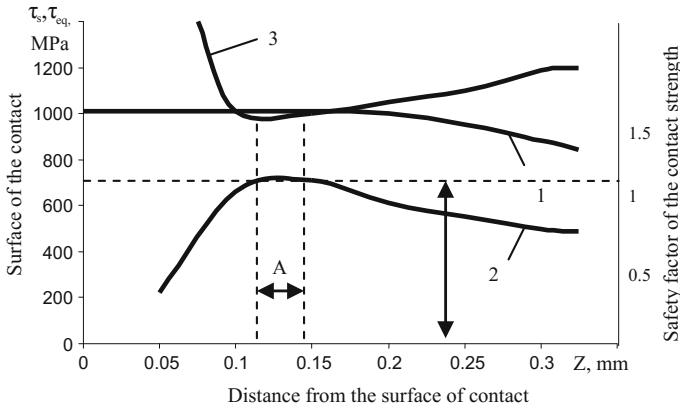


Fig. 11 Diagrams of stress distribution at the surface layer of bearing parts for a PTM under static loads (overloads) and the corresponding values of safety factors of the contact strength n in different zones of the contacting surface hardened by laser. A is the area where primary contact fractures can appear

Contacting parts with surface hardened layers have been subjected to analysis. The parts have the following characteristics of physical and mechanical properties: $E_o = E_u = 2.1 \times 10^5$ (MPa); Poisson's factors $\mu_o = \mu_u = 0.3$; hardness of the satellite axis core $H_c = 3500$ (MPa); surface hardness at case-hardening $H_n = 6200-7000$ (MPa); surface hardness at laser treatment $H_n = 8000-8500$ (MPa); the depth of the hardened layer at case-hardening $\delta_c = 0.7$ mm; the depth of the hardened layer at laser treatment $\delta_c = 0.5$ mm; radii of the curvature of contacting parts $R_o = 14.6$; $R_u = 2$ mm. The design value of the thrust in the contact is $F_{eq} = F_u = 10.5$ kN.

Strength analysis under cyclic loads has been performed for two cases of surface hardening: case-hardening and laser treatment. The design value of the thrust in the contact is $F_{eq} = F_u = 6.7$ kN.

The calculation results are shown in Figs. 12 and 13.

The diagrams show that the minimum values of the safety factor for the analyzed PTM are: for case-hardened parts of the bearing, $n_{min} \approx 1.1$, for parts hardened by laser, $n_{min} > 1.3$. This is stipulated by higher values allowable for parts hardened by laser ($\tau_s \approx 1000$ MPa, $\tau_k \approx 670$ MPa), which in turn are stipulated by a higher degree of hardness on the metal surface after laser hardening ($H_n = 8000-8500$ MPa). Moreover, the specific feature of laser hardening is the resulting high hardness being found practically throughout the entire depth of the hardened layer. Thus, for example, in the zone of action of maximum equivalent stresses at a depth of $z = 0.08-0.15$ mm, the laser-hardened layer possesses the high degree of hardness close to that of the surface. At the same time, at case-hardening and nitro-carburizing, the material of a part has a hardness at the zone of action of maximum equivalent stresses that is considerably lower than the surface hardness.

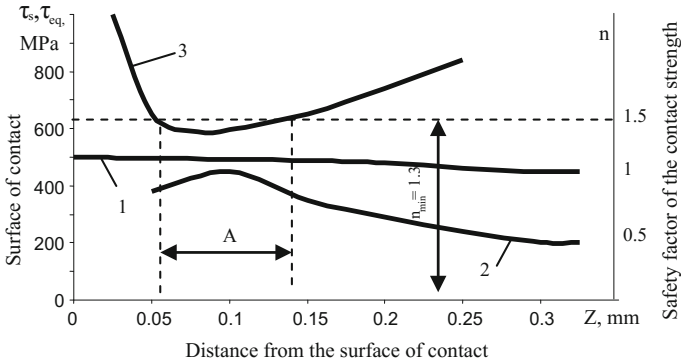


Fig. 12 Diagrams of stress distribution at the surface layer of bearing parts for a PTM under cyclic loads (overloads) and the corresponding values of safety factors of the contact strength n in different zones of the contacting surface that is case-hardened. A is the area where primary contact fractures can appear

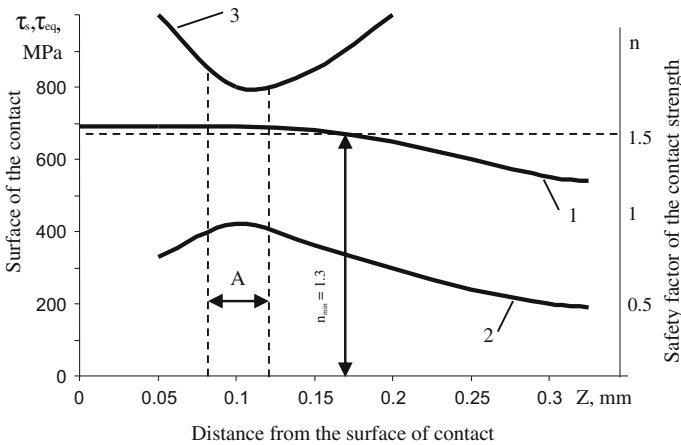


Fig. 13 Diagrams of stress distribution at the surface layer of bearing parts for a PTM under cyclic loads (overloads) and the corresponding values of safety factors of the contact strength n in different zones of the contacting surface hardened by laser. A is the area where primary contact fractures can appear

Experiments have shown that fatigue fractures in operating surfaces do not appear if the values of the safety factor in the risky zone are $n_{min} > 1.3$. Tests of case-hardened parts showed that if the condition $n_{min} > [n_{min}]$ is not fulfilled, the fractures appear at depths close to those of the design. Thus, at a depth of 0.07–0.14 mm, fatigue cracks have been detected that led to lamination of significant areas of the surface and failure of parts. Similar fractures have been detected when investigating the failed bearing parts for a PTM after long-term operation (more

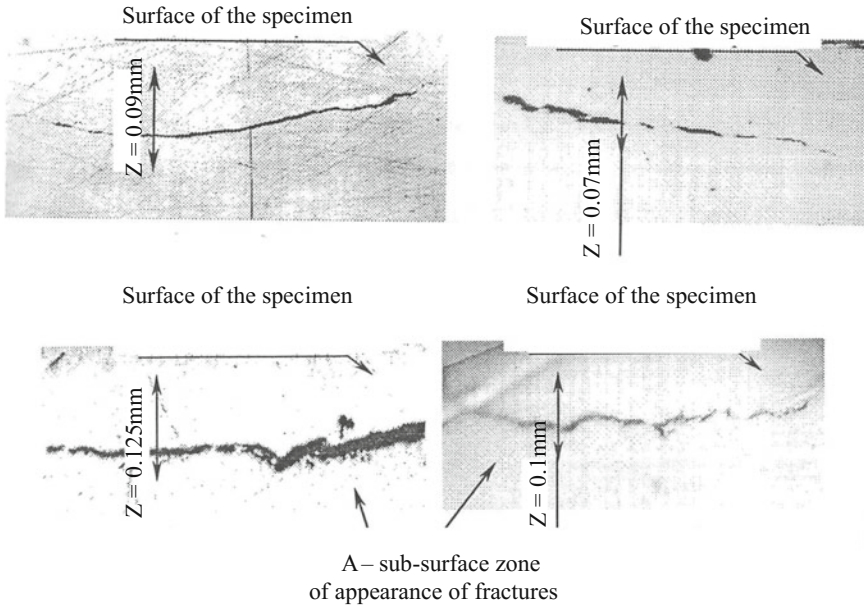


Fig. 14 Character of fractures and arrangement of fatigue cracks in the surface layer after stand tests

than 6000 motor hours). The character of fractures and cracks at the lateral micro-section is shown in Fig. 15. It is determined that the calculated depth of location of the risky zone (zone A, see Figs. 13 and 14) practically coincides with the zone of generation of sub-surface cracks revealed during the experimental study.

On the basis of the studies performed on the depth contact strength and load-carrying capacity of bearings for a PTM, a new method has been proposed for analysis of the depth contact strength of bearings. Its flow-chart is shown in Fig. 16.

The theoretical and experimental studies performed allowed for development of recommendations as to the choice of optimal properties of surface—hardened bearings that operate under the action of high contact loads.

It is recommended that the effective hardness H^{ef} , the effective thickness of the layer δ^{ef} and the relation δ^{ef}/δ_c (that is, the relation of the effective thickness of the layer to the total thickness of the hardened layer) be indicated in technical documentation as features of the properties of the surface layer, along with the surface hardness.

The effective thickness of the hardened layer, accounting for the provision of the required safety factor of the depth cyclic contact strength $n_{min} \geq 1.1$, is determined by the expression

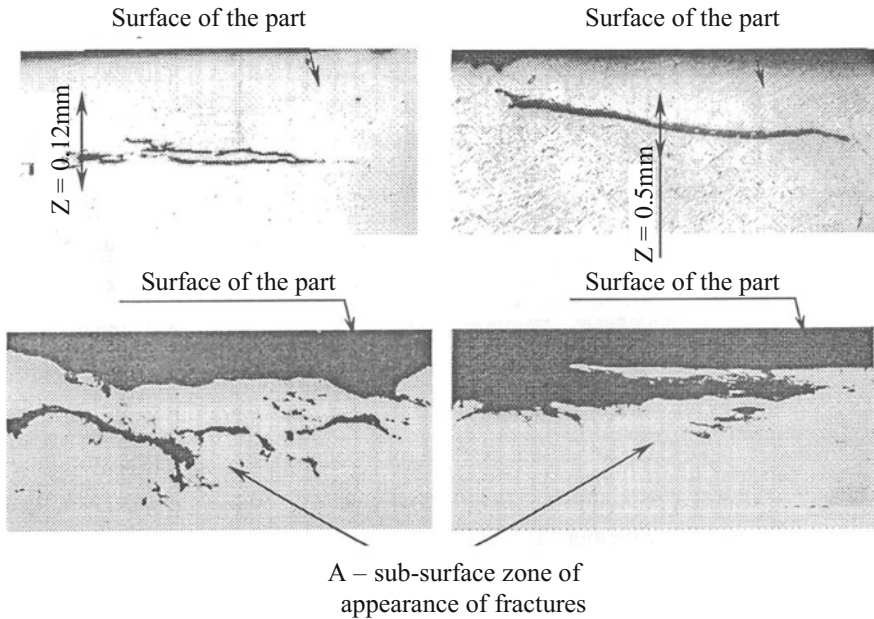


Fig. 15 Character of fractures and arrangement of fatigue cracks on parts that failed after long-term operation

$$\delta_y^{ef} = 1.386 \times 10^{-5} \sigma_n [n] \cdot p_{red}. \tag{11}$$

If the maximum stresses act under the hardened layer, the effective thickness of the hardened layer must be equal to the total thickness of the layer, that is, $\delta^{ef} = \delta_c$.

In order to prevent depth fractures at the boundary of the layer and the core (when the condition of the depth strength is fulfilled in the zone of maximum equivalent stresses at the thickness $z_{max} = \delta^{ef}$), it is necessary to provide the definite relation between the total δ_c and the effective δ^{ef} thicknesses of the hardened layer.

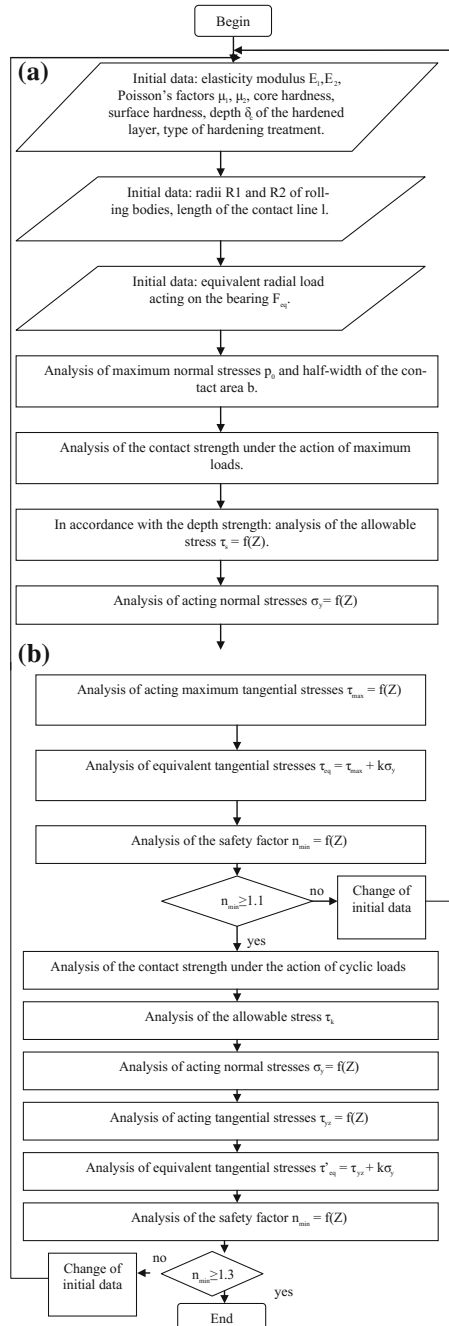
This relation is as follows:

$$\frac{\delta_c}{\delta_y^{ef}} = \sqrt{\frac{[n] \sigma_n - 4.1 H_c}{0.85 H_c}}. \tag{12}$$

The necessary hardness of the hardened layer at the thickness δ^{ef} can be determined by the equation that describes the hardness distribution $H(z)$ along the thickness of the case-hardened layer,

$$H^{ef} = \frac{H_n}{\left(\frac{H_n}{H_c} - 1\right) \cdot \left(\frac{\delta_y^{ef}}{\delta_c}\right) + 1}. \tag{13}$$

Fig. 16 Flow-chart of the analysis of the depth contact strength under the action of maximum loads (a) and cyclic loads (b)



In case of laser treatment,

$$H^{ef} = \frac{H_n}{\left(\frac{H_{mas}}{H_{cn}} - 1\right) \cdot \left(\frac{\delta_c^{ef}}{\delta_c}\right) + 1}. \quad (14)$$

The necessary value of H^{ef} should meet the requirement $H^{ef} \geq 0.22\sigma_H[n]$.

Therefore, the increase in the load-carrying capacity of surface-hardened rolling supports can be provided by the choice of the required characteristics of hardened layers. Application of the developed methods for analysis of contacting parts allows for calculating these characteristics in accordance with the condition of the depth contact strength.

On the basis of the investigation results and analysis, it is recommended that the following values of characteristics of hardened layers for heavy-loaded bearings for the planetary mechanism of the mobile machine be assigned:

$$H \geq 7500 \text{ MPa}; \delta^{ef} \geq 0.5; [n]_{min} \geq 1.5. \quad (15)$$

4 Conclusions

1. The analysis has been performed for the loading state of bearings for the planetary mechanism of the transmission; the factors that influence the serviceability of bearings and the criteria that determine the limiting state of operating surfaces have been revealed.
2. The mathematical model has been developed that describes the conditions of the contact loading of surface hardened bearings for power gears.
3. New methods have been developed for analysis of the contact strength of surface hardened bearings under static and cyclic loading. They are distinguished, since the design relations have been obtained accounting for the laws of stress variation from the surface to the core of the main metal. The analysis allows for determining not only the limiting contact stresses that do not cause fractures, but also the optimal characteristics of the surface layers of bearing parts (H^{ef} , δ_c^{ef} , H_n , H_c).
4. It is established that the angular twist of rolling bodies of the bearing for a PTM has an influence on the distribution of contact loads; and it is proposed that we take this fact into account by the factor k_γ . The technique for its determination has also been presented.
5. It is established that in order to provide the required safety factors of the depth strength, eliminate contact fractures and increase the durability of bearings for the planetary mechanism, the thickness of the hardened layer with the highest hardness ($H_\gamma > 8000 \text{ MPa}$) should be no less than 0.5 mm.

6. When testing bearings hardened by laser, the effect of self-organizing for friction surfaces has been revealed. It implies that the wave-like micro-relief “oil pockets” are generated on the surface during operation. This causes an increase in the oil absorption of the contact, an improvement in lubrication conditions (especially for transient modes), a decrease in the rate of wear and, correspondingly, an increase in durability. Therefore, the increase in the wear of bearing parts hardened by laser is achieved as a result of the total effect of optimization of properties of the hardened layer and improvement of the lubrication condition for transient modes. Laser treatment of operating surfaces is recommended as an effective method for increasing the load-carrying capacity of rolling bearings for power gears.

References

1. Pinegin, S.V.: Contact Strength and Resistance to Rolling. Mashinostroyeniye, Moscow (1969) (in Russian)
2. Saverin, M.M.: Contact Strength of the Material. Mashgiz, Moscow (1946) (in Russian)